Article

Cell Reports

Dual and Direction-Selective Mechanisms of Phosphate Transport by the Vesicular Glutamate Transporter

Graphical Abstract

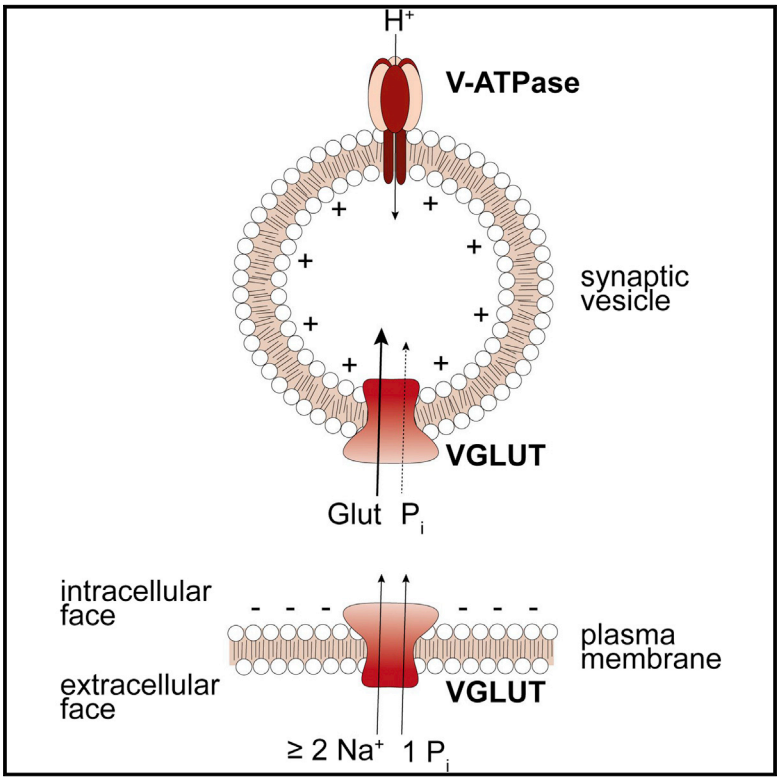

Highlights

- VGLUT transports phosphate ions (P_i) as alternative substrate in two modes
- P_i transport into synaptic vesicles is driven by an electrochemical proton gradient
- In the inverse orientation, P_i transport is coupled to Na^+ co-transport
- Different transport modes depend on flexible ion binding sites with changing affinities

Authors

Julia Preobraschenski, Cyril Cheret, Marcelo Ganzella, ..., Stephan Schenck, Reinhard Jahn, Gudrun Ahnert-Hilger

Correspondence

rjahn@gwdg.de (R.J.), gudrun.ahnert@charite.de (G.A.-H.)

In Brief

Preobraschenski et al. show that the vesicular glutamate transporter functions as a bi-directional phosphate transporter that is coupled with different cations in each direction and hence may play a key role in neuronal phosphate homeostasis.

Preobraschenski et al., 2018, Cell Reports *23*, 535–545
April 10, 2018
https://doi.org/10.1016/j.celrep.2018.03.055

CellPress

Cell Reports
Article

Dual and Direction-Selective Mechanisms of Phosphate Transport by the Vesicular Glutamate Transporter

Julia Preobraschenski,[1] Cyril Cheret,[2] Marcelo Ganzella,[1] Johannes Friedrich Zander,[2] Karin Richter,[2] Stephan Schenck,[3] Reinhard Jahn,[1,4,*] and Gudrun Ahnert-Hilger[2,*]
[1]Department of Neurobiology, Max-Planck-Institute for Biophysical Chemistry, 37077 Göttingen, Germany
[2]Institute for Integrative Neuroanatomy, Charité, Medical University of Berlin, 10115 Berlin, Germany
[3]Laboratory of Biomolecular Research, Paul Scherrer Institut, CH-5232 Villigen, Switzerland
[4]Lead Contact
*Correspondence: rjahn@gwdg.de (R.J.), gudrun.ahnert@charite.de (G.A.-H.)
https://doi.org/10.1016/j.celrep.2018.03.055

SUMMARY

Vesicular glutamate transporters (VGLUTs) fill synaptic vesicles with glutamate and are thus essential for glutamatergic neurotransmission. However, VGLUTs were originally discovered as members of a transporter subfamily specific for inorganic phosphate (P_i). It is still unclear how VGLUTs accommodate glutamate transport coupled to an electrochemical proton gradient $\Delta\mu H^+$ with inversely directed P_i transport coupled to the Na^+ gradient and the membrane potential. Using both functional reconstitution and heterologous expression, we show that VGLUT transports glutamate and P_i using a single substrate binding site but different coupling to cation gradients. When facing the cytoplasm, both ions are transported into synaptic vesicles in a $\Delta\mu H^+$-dependent fashion, with glutamate preferred over P_i. When facing the extracellular space, P_i is transported in a Na^+-coupled manner, with glutamate competing for binding but at lower affinity. We conclude that VGLUTs have dual functions in both vesicle transmitter loading and P_i homeostasis within glutamatergic neurons.

INTRODUCTION

Signaling between neurons is mediated by the exocytotic release of neurotransmitters from synaptic vesicles (SVs) in presynaptic nerve endings. The released transmitter activates postsynaptic receptors and is then rapidly cleared by Na^+-dependent transporters located in the plasma membrane of surrounding neurons and astrocytes. The membrane of SVs is retrieved by endocytosis. SVs are regenerated in the nerve terminal and re-filled with transmitters from cytoplasmic pools (Sudhof, 2004).

Neurotransmitter uptake by SVs is driven by an electrochemical proton gradient ($\Delta\mu H^+$) generated by a vacuolar proton ATPase (Ahnert-Hilger et al., 2003; Edwards, 2007). Eight transporters, belonging to three subfamilies of solute carriers (SLC17, SLC32, and SLC18, respectively) are known. Substrate specificities and transport mechanisms vary among the subfamilies, because the transmitters have different net charges, thus requiring distinct ion-coupling mechanisms (Omote et al., 2011). Moreover, the transporters must maintain efficient uptake not only when a vesicle is empty, i.e., filled with extracellular electrolytes acquired during endocytosis, but also when a vesicle is partially filled, with transmitter concentrations well exceeding 100 mM requiring highly adaptive transport mechanisms (Farsi et al., 2017) (Takamori, 2016).

The ionic mechanism or mechanisms by which SVs are filled with glutamate, the main excitatory neurotransmitter of the mammalian CNS, are only partially understood. Transport is electrogenic and activated by chloride ions at low millimolar concentrations (Maycox et al., 1988; Naito and Ueda, 1985; Tabb et al., 1992), which appear to bind to a regulatory site distinct from the substrate binding site (Hartinger and Jahn, 1993; Juge et al., 2010; Wolosker et al., 1996). However, it has been a major challenge to understand how transport is coupled to the electrochemical proton gradient and which ions are involved. Research indicates that vesicular glutamate transporters (VGLUTs) can translocate both monovalent anions and cations, but coupling appears to be loose, i.e., allowing for variable stoichiometry and thus for operation in different transport modes that gradually change during vesicle filling (Preobraschenski et al., 2014). When a vesicle is empty, the glutamate anion is translocated either alone or in exchange for a proton, explaining the almost-exclusive dependence on an inside positive membrane potential. Moreover, glutamate uptake may be linked to chloride export, but not stoichiometrically (Preobraschenski et al., 2014; Schenck et al., 2009). In this mode, the negative charge of glutamate is balanced by proton import catalyzed by the vacuolar-type H^+-ATPase (V-ATPase), i.e., transport results in the net uptake of glutamic acid. When the buffering capacity of SVs (25–70 mM) (Egashira et al., 2015; Farsi et al., 2016) is exhausted, a second transport mode of VGLUT becomes relevant that involves exchange of a lumenal H^+ with cytoplasmic K^+. In addition, SVs contain a Na^+/H^+ exchanger NHE6 (Grønborg et al., 2010; Orlowski and Grinstein, 2004) that, together with the K^+/H^+ exchange activity of VGLUT, ensures charge-neutral proton exit and thus prevents over-acidification of the vesicle lumen while accumulating high concentrations of glutamate (Goh et al., 2011; Preobraschenski et al., 2014).

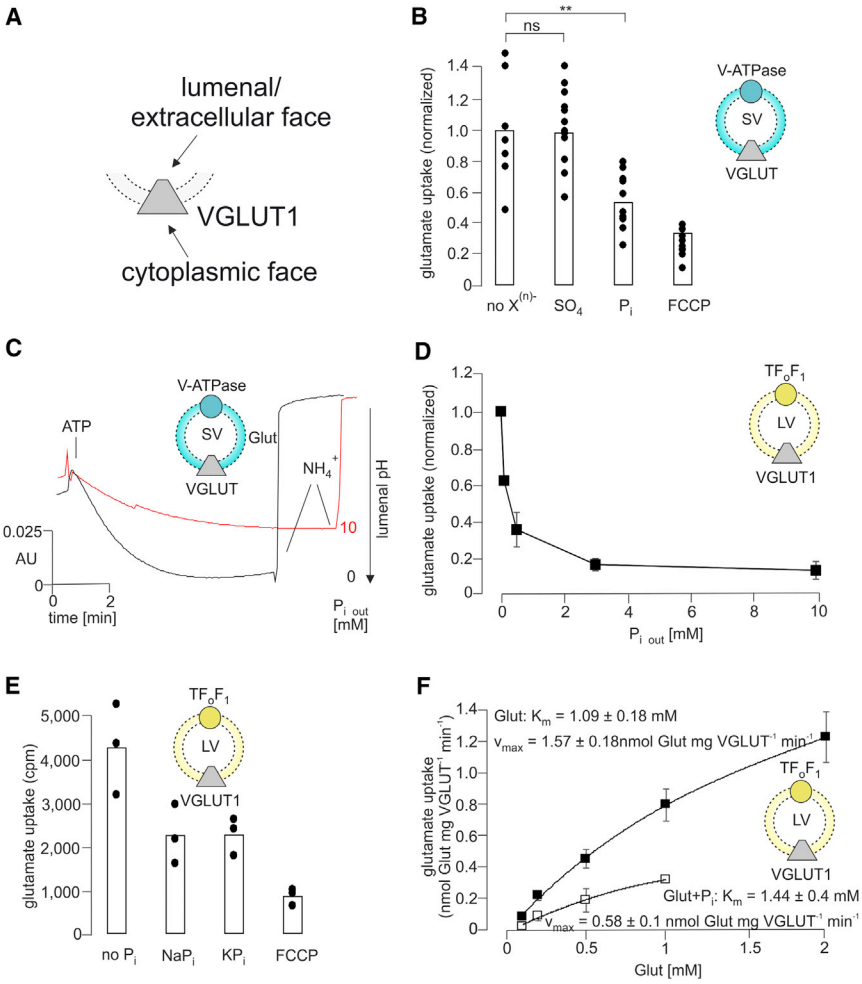

Figure 1. Influence of P_i on Glutamate Uptake and Glutamate-Dependent Acidification

(A) Scheme explaining the two faces of VGLUT1 shown in the subsequent panels.

(B) P_i, but not sulfate ions, reduce glutamate uptake by SV. Uptake was performed in the presence of 2 mM ATP, 4 mM KCl (no $X^{(n)-}$), and where indicated, 10 mM potassium phosphate (P_i) or potassium sulfate (SO_4) in 150 mM K-gluconate uptake buffer and 30 μM of the proton ionophore Carbonyl cyanide-4-(trifluoromethoxy)phenylhydrazone (FCCP). Data were normalized to the no $X^{(n)-}$ condition and were analyzed using a two-tailed paired t test, $^{**}p < 0.01$ ($p = 0.002$), and NS (not significant, $p > 0.05$).

(C) ATP-dependent acidification in the presence of 10 mM glutamate (Glut) is reduced in the presence of 10 mM P_i ($P_{i\ out}$). Acidification was measured using acridine orange as reporter dye. The measurements were performed in 150 mM Na-gluconate buffer, and the osmolarity was kept constant by replacing sodium gluconate with P_i. A decrease in absorbance reflects acidification.

(D) Dependence of glutamate uptake by VGLUT1/TF_oF_1 liposomes on the external P_i concentration ($P_{i\ out}$). Data were normalized to the condition without P_i.

(E) Glutamate uptake by VGLUT1/TF_oF_1 proteoliposomes in the presence of 10 mM potassium phosphate (KP_i) and sodium phosphate (NaP_i) and 30 μM FCCP. Unless indicated otherwise, glutamate uptake was measured after 15 min in these and all subsequent experiments.

(F) Kinetics of glutamate uptake by VGLUT1/TF_oF_1 proteoliposomes preloaded with glycine buffer performed under standard conditions (black squares) and in the presence of 300 μM P_i (white squares). The glutamate concentration was adjusted with non-labeled substrate, while ^{3}H-labeled glutamate was kept constant. Data were corrected for uptake in the presence of FCCP.

Black circles in (B) and (E) indicate individual data points. Error bars represent the experimental range (D) or SEM (F). n = 4–9 (B), 1–2 (D), 3 (E), and 2–5 (F).

VGLUTs were originally discovered as coupled Na^+/inorganic phosphate (P_i) co-transporters (Aihara et al., 2000; Ni et al., 1994) similar to other members of the SLC17 family (Busch et al., 1996). It is unclear how these two transport activities are related to each other and to which extent the substrate binding sites overlap. It has been suggested that glutamate and phosphate transport are independent of each other (Juge et al., 2006). However, in these experiments, the orientation of the transporter was not controlled. Thus, it remains unclear whether the two transport activities occur in opposite directions (as one would expect) and how Na^+ ions that have no role in glutamate transport are linked to phosphate uptake.

In the present study, we aim to clarify, using multiple and independent approaches, whether and under which conditions VGLUT transports P_i and how P_i transport relates to glutamate transport. Our data suggest that VGLUT can function as a $\Delta\mu H^+$-dependent P_i transporter in the SV orientation and as an electrogenic Na^+-dependent P_i transporter in the plasma membrane orientation, using the same anion binding site for both phosphate and glutamate.

RESULTS

P_i Inhibits VGLUT-Mediated Glutamate Uptake and Glutamate-Dependent Acidification

First, we tested whether P_i influences glutamate uptake by purified SVs (see Figure 1A for a depiction of VGLUT orientation). Addition of P_i substantially reduced glutamate uptake, in contrast to sulfate (Figure 1B), in line with previous reports (Naito and Ueda, 1985). Next, we tested whether P_i inhibits glutamate-dependent acidification of the vesicle lumen. As outlined earlier, protons serve as counter-ions for glutamate uptake during the initial phase of vesicle loading and thus provide an indirect measure for glutamate uptake. 10 mM P_i reduced glutamate-dependent acidification of SV (Figure 1C).

To examine whether the inhibitory effect of P_i on glutamate uptake is due to a direct interaction with VGLUT1, we reconstituted purified VGLUT1 in liposomes, together with a bacterial proton ATPase (TF_oF_1) (Preobraschenski et al., 2014). As shown in Figure 1D, P_i inhibited glutamate uptake by VGLUT liposomes

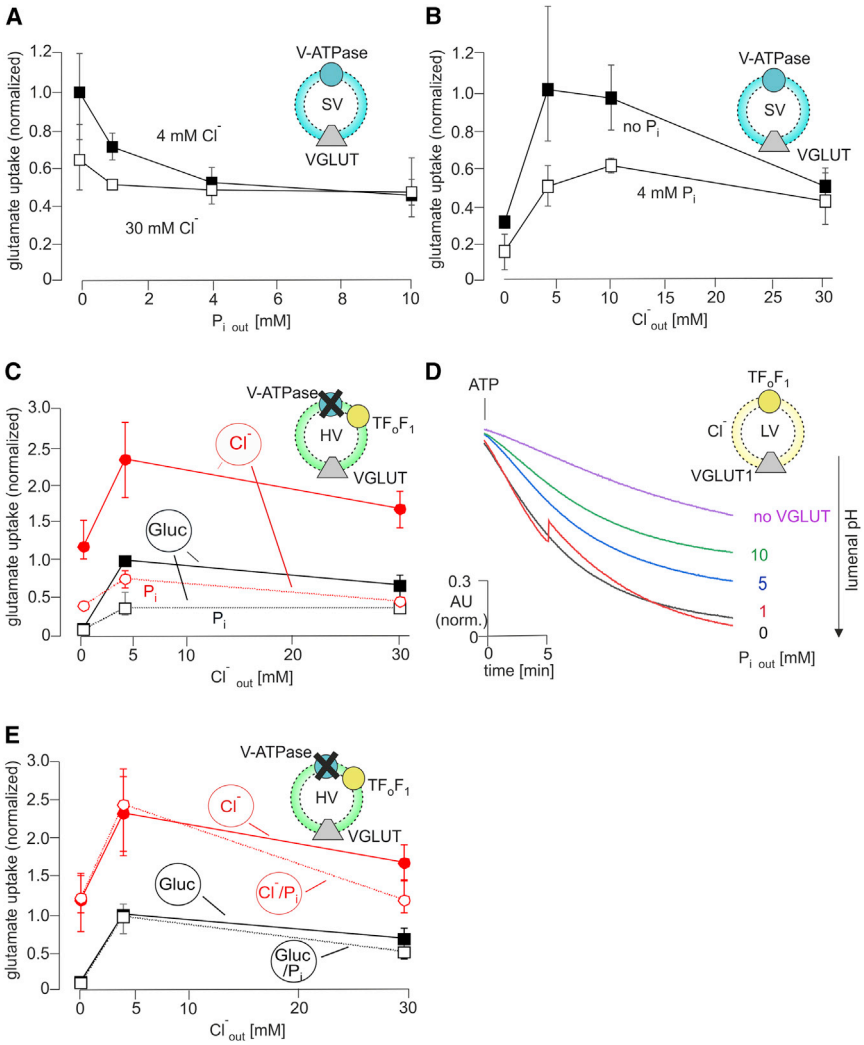

Figure 2. P_i Inhibits Glutamate Uptake Independent of Cl^-, but Only when Present on the outside (Cytoplasm-Facing Side) of the Vesicles

(A) Glutamate uptake by SV is inhibited by increasing P_i concentrations both at low (4 mM) and high (30 mM) chloride (Cl^-) concentrations.

(B) Biphasic dependence of glutamate uptake by SV on the external Cl^- concentration is preserved in the presence of P_i (4 mM). Uptake in (A) and (B) was performed in K-gluconate buffer. Data were normalized to uptake at 4 mM Cl^- in the absence of P_i.

(C) Glutamate uptake by hybrid vesicles (HVs) generated by fusing SVs with TF_oF_1 liposomes preloaded with either 150 mM choline chloride (Cl^-, red lines) or choline gluconate (Gluc, black lines). Uptake was measured at increasing external Cl^- concentrations in the presence (open symbols) and absence (filled symbols) of 10 mM P_i.

(D) Acidification of VGLUT1/TF_oF_1 liposomes preloaded with 300 mM glycine buffer in the presence of 30 mM Cl^- at increasing P_i concentrations. The reaction was initiated by addition of 1.2 mM ATP. Measurements were performed in glycine buffer.

(E) Glutamate uptake is not influenced by lumenal P_i, regardless of the presence of external Cl^-. Uptake was measured using hybrid vesicles preloaded with reconstitution buffer containing 150 mM choline gluconate (Gluc, black line), 120 mM choline gluconate and 30 mM P_i (Gluc/P_i, dashed black line), 150 mM choline chloride (Cl^-, red line), or 120 mM choline chloride and 30 mM P_i (Cl^-/P_i, dashed red line).

Data in (C) and (E) were normalized to uptake by Gluc-preloaded hybrid vesicles at 4 mM Cl^-. Error bars represent the experimental range. n = 2–8 (A), 3–7 (B), 1–6 (C), and 3–6 (E).

in a dose-dependent manner, with maximal inhibition attained ~3 mM P_i. Inhibition by P_i was observed, regardless of whether K^+ or Na^+ was used as a counter-ion (Figure 1E). Similar observations were made in parallel experiments carried out with purified SV (Figure S1A).

To analyze whether P_i inhibits glutamate uptake in a competitive manner, we measured glutamate uptake into VGLUT liposomes at varying glutamate concentrations in the absence and presence of 300 μM P_i (half maximal inhibitory concentration [IC_{50}]) and determined the transport kinetics. The affinity and maximal transport rate for glutamate were significantly reduced in the presence of P_i (K_m (glutamate [Glut]) = 1.09 ± 0.18 mM, V_{max} = 1.57 ± 0.18 nmol Glut mg $VGLUT^{-1}$ min^{-1} and K_m (Glut+P_i) = 1.44 ± 0.4 mM, V_{max} = 0.58 ± 0.1 nmol Glut mg VGL^{-1} min^{-1}) (Figure 1F), strongly suggesting a competitive inhibition of glutamate transport by P_i.

To exclude that the concentrations of P_i used here affect the electrochemical proton gradient, we carried out two control experiments. First, we compared the effect of P_i on vesicular glutamate uptake with that on vesicular γ-aminobutyric acid (GABA) and 5-hydroxytryptamine (5-HT) uptake. Only glutamate uptake was significantly reduced by P_i (Figure S1B), showing that inhibition is not caused by an impairment of the driving force. Second, we measured lumenal acidification by TF_oF_1 ATPase reconstituted in liposomes in the presence of varying concentrations of P_i. Only slightly reduced acidification was observable at P_i concentrations up to 10 mM (Figure S1C).

P_i Competes with Cl^- for the Substrate Binding Site of VGLUT in the SV Orientation

In the SV orientation, VGLUT exhibits a substrate binding site that prefers glutamate over chloride and a regulatory binding site for chloride that activates glutamate transport at low Cl^- concentrations (see the Introduction) (Preobraschenski et al., 2014; Wolosker et al., 1996). We therefore tested whether P_i-mediated inhibition of glutamate uptake is caused by interference with one or both of these binding sites.

First, we measured glutamate uptake by SV at varying P_i concentrations in the presence of either 4 or 30 mM Cl^-. In both cases, maximal inhibition was observed at 4 mM P_i, but the

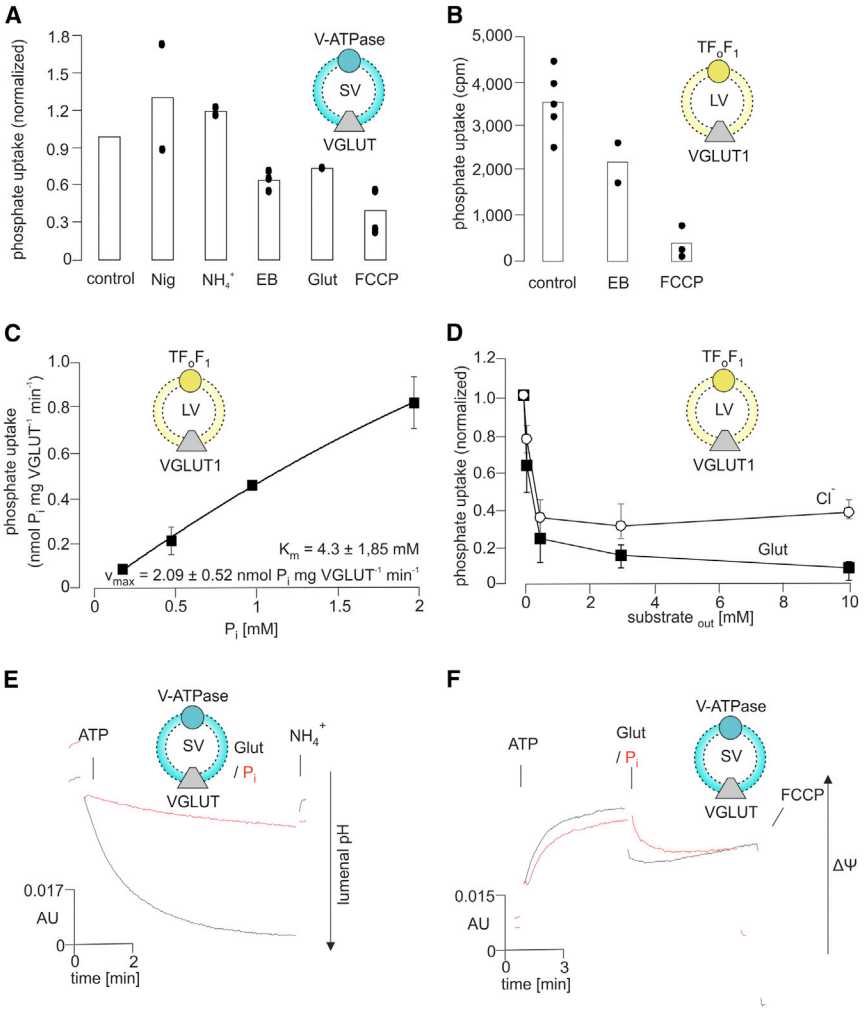

Figure 3. VGLUT Transports P_i in a $\Delta\mu H^+$-Dependent Manner

(A) P_i uptake by SV in the presence of 4 mM ATP (control). Uptake was enhanced in the presence of 5 nM nigericin and 10 mM NH_4^+ and inhibited by 1 μM Evans blue (EB), 10 mM non-labeled glutamate, and 30 μM FCCP. Data were normalized to the control condition.

(B) P_i uptake by VGLUT1/TF_oF_1 liposomes in the presence of 4 mM ATP (control) using a standard K-gluconate uptake buffer. Uptake was sensitive to Evans blue (EB) and FCCP. Data were corrected for background counts in samples containing liposomes reconstituted in the absence of VGLUT.

(C) Kinetics of P_i uptake by VGLUT1/TF_oF_1 proteoliposomes preloaded with glycine buffer performed under standard conditions. The P_i concentration was adjusted with non-labeled substrate, while ^{33}P-labeled P_i was kept constant. Data were corrected for uptake in the presence of FCCP.

(D) Graph shows that P_i uptake by VGLUT1/TF_oF_1 liposomes is progressively inhibited by increasing glutamate and chloride (Cl^-) concentrations. Data were corrected for uptake in the presence of FCCP and normalized to the condition in the absence of glutamate and chloride.

(E and F) The influence of P_i (red line) and glutamate (black line) on lumenal acidification (E) and inside positive membrane potential (F) in SV. Proton pumping by the endogenous V-ATPase was initiated by addition of 1.2 mM ATP. The measurements were performed in 150 mM Na-gluconate buffer. P_i, unlike glutamate, does not cause acidification but resembles glutamate in its dissipative effect on $\Delta\Psi$.

Black circles indicate individual data points. Error bars represent SEM (C) or the experimental range (D). n = 1–3 (A), 2–5 (B), 2 (C), and 1–3 (D).

relative inhibition was more pronounced in the presence of 4 mM Cl^-, rather than 30 mM Cl^- (Figure 2A). Therefore, we measured the effect of 4 mM P_i on glutamate uptake in the presence of increasing Cl^- concentrations (Figure 2B). Although glutamate uptake was reduced by P_i at all Cl^- concentrations, the profile of Cl^- dependence was maintained in the presence of P_i (Figure 2B). These data suggest that P_i primarily competes with the substrate binding site.

Next, we tested whether P_i inhibits vesicular glutamate loading if uptake is enhanced by the presence of Cl^- ions inside the lumen of the vesicles (Preobraschenski et al., 2014; Schenck et al., 2009). For these experiments, we fused SVs with TF_oF_1-containing liposomes containing 150 mM Cl^-, resulting in hybrid vesicles (Preobraschenski et al., 2014). Although glutamate uptake was enhanced as expected (Figure 2C), external addition of 10 mM P_i resulted in pronounced inhibition, regardless of the external Cl^- concentration (Figure 2C). Similar observations were made using liposomes reconstituted with purified VGLUT (Figure S2A). Altogether, these data are best interpreted as a competition by P_i of glutamate binding on the substrate binding site facing the cytoplasm.

VGLUT also exhibits chloride conductance (Bellocchio et al., 2000; Eriksen et al., 2016; Preobraschenski et al., 2014; Schenck et al., 2009). This conductance can be indirectly detected by lumenal acidification of VGLUT/TF_oF_1 liposomes, because Cl^- ions serve as counter-ions for the electrogenic proton pump (Preobraschenski et al., 2014; Schenck et al., 2009). As shown earlier, Cl^--dependent acidification is mitigated by glutamate, suggesting chloride translocation through the substrate binding site (Bellocchio et al., 2000; Preobraschenski et al., 2014). Thus, we tested whether P_i inhibits Cl^--dependent acidification. At 30 mM chloride, P_i inhibited acidification in a dose-dependent manner, suggesting competition for the substrate binding site (Figure 2D). A similar observation was made with purified SV (Figure S2B).

Finally, we investigated whether glutamate uptake was affected when P_i was present in the vesicle lumen using hybrid vesicles (Figure 2E) or VGLUT liposomes (Figure S2C). No significant inhibition was observable, regardless of whether intravesicular Cl^- was present (Figure 2E).

In summary, cytoplasmic P_i interferes with glutamate translocation mainly by binding to the substrate binding site of VGLUT

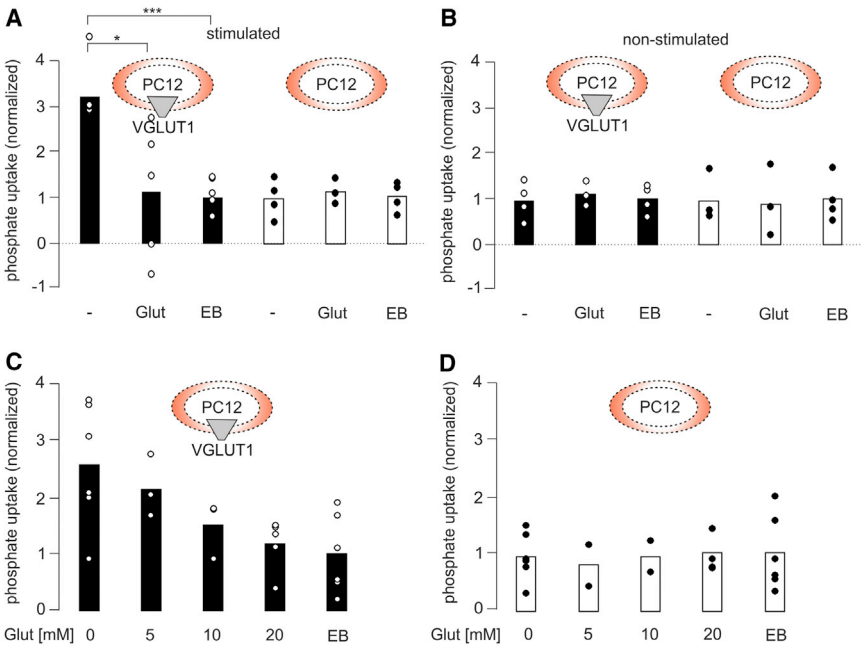

Figure 4. PC12 Cells Expressing Heterologous VGLUT1 Accumulate P_i in a Na^+-Dependent Manner

Na^+-dependent P_i uptake by PC12 cells expressing VGlut1 or transfected with empty vector (control).

(A and B) Phosphate uptake by PC12 cells that were either depolarized by 30 mM KCl to stimulate exocytosis (in the presence of 80 μM dynasore to block compensatory endocytosis) (A) or remained non-stimulated (B). Uptake was measured by determining the cellular phosphate content with a colorimetric assay at the end of the incubation. All assays were carried out with a substrate concentration of 10 mM (NaP_i) in the presence of 50 mM $NaCl^-$ and complemented with 20 mM Na-gluconate (Na^+) (replaced with 20 mM Na-glutamate [Glut] where indicated). The VGLUT inhibitor Evans blue (EB) was added at 2μM.

(C and D) Response of Na^+-dependent P_i uptake in stimulated VGlut1 (C) or control (mock-transfected) (D) cells to increasing concentrations of glutamate and 2 μM Evans blue (EB).

Data were normalized to the respective Evans Blue treatment conditions. Independent experimental values are indicated by white (VGLUT1) or black (mock) circles. n = 3–6 (A), 3–4 (B), 3–6 (C), and 2–6 (D). Data in (A) were analyzed using a two-tailed paired t test, *$p < 0.05$ ($p = 0.01$), and ***$p < 0.001$ ($p = 0.00003$).

facing the cytoplasm. Because stimulation by 4 mM Cl^- of glutamate uptake is maintained in the presence of P_i, an interference of P_i with the regulatory chloride binding site is less likely but cannot be ruled out.

VGLUT Transports P_i as Alternative Substrate in a $\Delta\mu H^+$-Dependent Manner

In the next experiments, we tested whether P_i is transported by VGLUT as an alternative substrate. We observed robust vesicular accumulation by SVs of P_i, which was sensitive to the proton uncoupler carbonyl cyanide-4-(trifluoromethoxy) phenylhydrazone (FCCP). Uptake was partially inhibited by the specific VGLUT inhibitor Evans blue or by an excess of non-labeled glutamate (Figure 3A). Nigericin and NH_4^+, which both increase $\Delta\Psi$ and therefore stimulate glutamate transport (Preobraschenski et al., 2014), enhanced P_i uptake, arguing for $\Delta\Psi$ as the primary driving force (Figure 3A). A similar profile was obtained when VGLUT liposomes were used instead of SVs (Figure 3B). ATP-dependent P_i uptake followed a time course comparable to standard *in vitro* glutamate uptake (Figure S3) (Maycox et al., 1988). Kinetic analysis of ATP-driven P_i uptake yielded an apparent K_m of 4.3 ± 1.85 mM and a V_{max} of 2.09 ± 0.52 nmol P_i, mg $VGLUT^{-1}$ min^{-1} which corresponds to a roughly 3-fold lower affinity for P_i than for glutamate (Figure 3C; see also Figure 1F).

To further explore the relative affinities of glutamate, chloride, and P_i, we measured P_i uptake in the presence of increasing concentrations of glutamate and Cl^-. In both cases, P_i transport was strongly reduced by low concentrations of each ion, with glutamate being more potent (Figure 3D), suggesting an apparent affinity of the substrate binding site in the order glutamate > Cl^- > P_i. In contrast to glutamate transport, however, we did not observe stimulation by low chloride concentrations of P_i transport (Figure 3D). The regulatory anion binding site is probably not accessible or functional if P_i is bound to the substrate binding site.

We additionally tested whether P_i transport is associated with a net translocation of protons. However, P_i (in the absence of other anions) resulted only in a minor acidification of SVs (Figure 3E). The lack of net acidification may be due to increased buffering by the imported P_i (pK_{a2} for P_i = 7.21). In contrast, P_i transport reduced $\Delta\Psi$ similar to glutamate (albeit with slower kinetics) (Figure 3F), indicating that for both substrate anions, $\Delta\Psi$ serves as the main driving force for uptake.

VGLUT Mediates Na^+-Coupled P_i Transport in the Plasma Membrane Orientation Using the Glutamate Binding Site

VGLUTs were originally identified as Na^+-coupled P_i transporters (Aihara et al., 2000; Ni et al., 1994), and it has been suggested that phosphate and glutamate transport are independent of each other (Juge et al., 2006). Considering that P_i and glutamate compete for the same binding site at the cytoplasmic face of the transporter, we decided to re-investigate the interactions among the different ions in the inverse (plasma membrane) orientation of the transporter.

First, we examined whether exogenous VGLUT1 mediates Na^+-dependent P_i accumulation. When expressed in PC12 cells, VGLUT is sorted into secretory vesicles that can be stimulated by K^+ depolarization to fuse with the plasma membrane. As shown in Figures 4A and 4B, P_i uptake was significantly enhanced after stimulation. No such enhancement was observable when

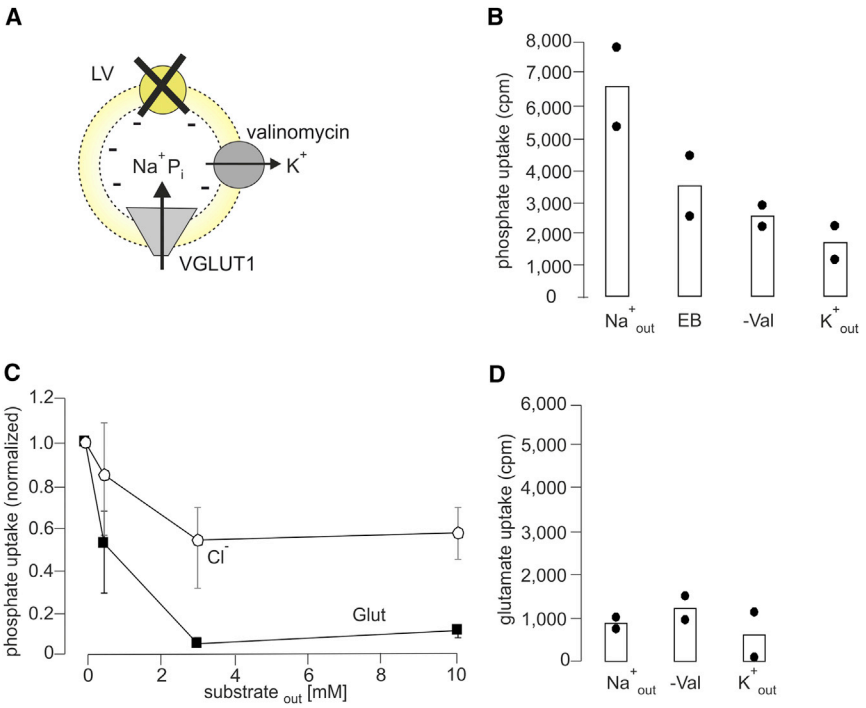

Figure 5. VGLUT Functions as Coupled Na^+/P_i Transporter in the Presence of an Inside Negative Membrane Potential

(A) Scheme showing the experimental system: VGLUT1-expressing liposomes were preloaded with 150 mM K-gluconate. P_i uptake was measured after an exchange of the external buffer with Na-gluconate. The K^+-selective ionophore valinomycin (3 nM) was added to generate an inside negative diffusion potential.

(B) P_i uptake, measured 1 min after addition of ^{33}P-labeled P_i (500 μM) in the presence of 150 mM external Na-gluconate and 3 nM valinomycin (Na^+_{out}). Uptake was inhibited by 1 μM Evans blue (EB), but not stopped, because uptake was higher than in the absence of valinomycin (−Val). Uptake was also reduced when Na-gluconate was replaced with K-gluconate (K^+). Data were corrected for uptake by liposomes lacking VGlut1.

(C) Na^+-dependent P_i uptake by VGLUT1 liposomes is inhibited by chloride (Cl^-) and glutamate. Data were corrected for uptake in the absence of valinomycin and normalized to the condition in the absence of glutamate or chloride.

(D) Glutamate uptake (1 min) into VGLUT1 liposomes preloaded with 150 mM K-gluconate in the presence of 150 mM Na-gluconate and 3 nM valinomycin (Na^+_{out}), in the presence of 150 mM K-gluconate and valinomycin (K^+_{out}), and in the absence of valinomycin (−Val). Data were corrected for uptake by liposomes lacking VGLUT1.

Black circles indicate individual data points. Error bars represent the experimental range. n = 2 (B), 5–8 (C), and 2 (D).

mock-transfected cells were used. Enhancement depended on Na^+ and was inhibited by Evans blue. These data confirm that VGLUT, when localized in the plasma membrane, functions as a Na^+-dependent P_i transporter.

P_i uptake was inhibited by glutamate (Figure 4A), with half-maximal inhibition between 5 and 10 mM (Figure 4C), but only in stimulated cells expressing VGLUT. This shows, contrary to a previous report (Juge et al., 2006), that glutamate competes with P_i in the reverse transport direction (Figures 4C and 4D). Apparently, both ions use an identical, or at least overlapping, binding site.

For additional confirmation, we resorted to VGLUT liposomes. We have shown that during reconstitution, a small fraction of the transporter (10%) is incorporated in the inverted orientation (Preobraschenski et al., 2014), i.e., with the lumenal (extracellular) side facing the outside of the liposome, thus allowing the inverse transport direction to be addressed using the same reconstitution protocol. Because Na^+-dependent P_i uptake requires an inside negative membrane potential (Forster et al., 1998, 2013), we preloaded the liposomes with high K^+ concentrations (150 mM) and then added the K^+ ionophore valinomycin (Figure 5A) (Parker et al., 2014). In the presence of external Na^+ (150 mM), we observed robust P_i accumulation (Figure 5B). Uptake depended on the presence of VGLUT, reduced in the absence of valinomycin or in the presence of Evans blue and almost abolished if K^+ was substituted for Na^+ (Figure 5B).

These data confirm that VGLUT catalyzes Na^+-dependent uptake of P_i. Because transport depends on both Na^+ and an inside negative membrane potential, we conclude that Na^+ serves as a counter-ion during transport, which results in the translocation of net positive charge. At physiological pH, P_i has an average charge of ~1.5 (pK_{a2} = 7.21). This suggests stoichiometry of ≥2 Na^+:1 P_i, although we do not know whether the mono- or the divalent P_i anion is transported.

Using this system, we next tested whether P_i binding in the plasma membrane orientation is affected by glutamate or Cl^-. Increasing concentrations of each ion resulted in progressive inhibition of Na^+-dependent P_i transport (Figure 5C). However, when compared to $\Delta\mu H^+$-driven P_i uptake in the inverse orientation, inhibition of Na^+-driven P_i transport was less pronounced and required higher concentrations for each ion (~3 versus 0.5 mM) to reach the maximal effect (compare Figure 3D and 5C). In particular, Cl^- was only partially inhibitory even at higher concentrations. This suggests that (1) the binding affinity for P_i is higher than that for glutamate and Cl^- in the Na^+-coupled transport direction and (2) in contrast to glutamate, Cl^- only partially interferes with the P_i binding site. The latter explains why VGLUT, when localized at the plasma membrane, can import net P_i despite high extracellular Cl^- concentrations. No glutamate transport was observable when VGLUT is in the plasma membrane orientation (Figure 5D), suggesting that its affinity is too low to be transported under physiological conditions.

For confirmation, we studied uptake under conditions in which VGLUT is exclusively in the SV orientation. To this end,

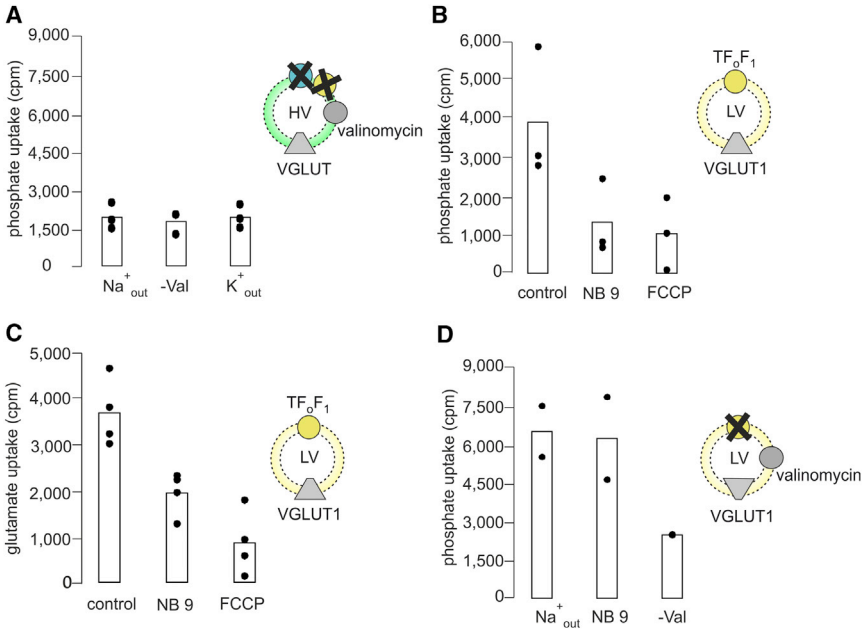

Figure 6. Na^+-Coupled P_i Transport by VGLUT Requires Plasma Membrane Orientation

(A) In contrast to VGLUT liposomes, no Na^+-coupled P_i uptake is measured when using hybrid vesicles that contain VGLUT exclusively in the SV orientation. Hybrid vesicles were preloaded with 150 mM K-gluconate and incubated in 150 mM external Na-gluconate in the presence of 3 nM valinomycin. No difference was observed, regardless of whether valinomycin was present (Na^+_{out}) or not (−Val) or whether extravesicular Na-gluconate was replaced by 150 mM K-gluconate (K^+_{out}).

(B and C) $\Delta\mu H^+$-dependent P_i uptake (B) and glutamate uptake (C) by VGLUT/TF_oF_1 liposomes are inhibited by a nanobody (NB 9) specific for the cytoplasmic domain of VGLUT1 in the SV orientation. The molar ratio between VGLUT1 and NB9 was adjusted to approximately 1:1 (mol/mol).

(D) In contrast, Na-coupled P_i uptake by VGLUT1 liposomes is not affected by NB 9 (see Figure 5 for details).

All data were corrected for uptake in liposomes reconstituted without VGLUT1. Black circles represent individual data points. n = 3 (A and B), 4 (C), and 2 (D).

we used hybrid vesicles that can be loaded with high K^+ while preserving the orientation of the transporter. Contrary to VGLUT liposomes, no Na^+-dependent P_i uptake was detectable (Figure 6A). As a second approach, we added a recently developed nanobody that binds to VGLUT solely in its SV orientation and inhibits glutamate transport (Schenck et al., 2017). $\Delta\mu H^+$-driven uptake of both P_i and glutamate by VGLUT liposomes was markedly reduced in the presence of the nanobody (Figures 6B and 6C), whereas Na^+-driven P_i uptake was not affected (Figure 6D).

Altogether, our data demonstrate that VGLUT operates as a coupled electrogenic Na^+-dependent P_i transporter. Both glutamate and phosphate bind to a single substrate binding site and thus compete with each other, but the relative binding affinities are in opposite order between the two sides of the transporter.

DISCUSSION

Using complementary approaches, we have demonstrated that VGLUT1 can transport P_i in opposite directions using two electrogenic but distinct transport mechanisms. In the SV orientation, VGLUT uses $\Delta\mu H^+$ to accumulate P_i, associated with translocation of net negative charge. In the plasma membrane orientation, P_i transport is coupled to the inwardly directed Na^+ gradient, associated with translocation of net positive charge. A single binding site appears to be used for all anionic substrates in both transport directions, which changes its substrate preferences during conformational switching. When considering the physiological ion concentrations in the cytoplasm and in the extracellular fluid, the properties of VGLUT are fully compatible with a dual role in glutamatergic neurons that solely depends on its localization: filling the vesicle with glutamate when localized in the SV membrane and importing phosphate when localized in the plasma membrane.

Our findings can be easily integrated into our previously proposed model for the VGLUT transport mechanism (Preobraschenski et al., 2014), which has been supported by studies (Eriksen et al., 2016; Farsi et al., 2016). According to this model, the transporter contains a regulatory and a substrate anion binding site and, based on the newly acquired data, one or more cation binding sites (Figure 7).

Like all secondary active transporters (Drew and Boudker, 2016; Forrest and Rudnick, 2009; Krishnamurthy et al., 2009), VGLUT shuttles between two main conformational states, with the substrate binding pocket open either to the cytoplasm (state I) or to the lumen of SV or the extracellular milieu (state II). When localized in SV, the binding pocket in state I recruits the substrate from the cytoplasm and releases it to the lumen of the SV after the transition to state II. When localized in the plasma membrane, the binding pocket is accessible to the extracellular milieu (state II), recruits the substrate from the extracellular fluid, and releases it into the cytoplasm after returning to state I. Reconstitution of VGLUT in liposomes allows for addressing both orientations in the same preparation (Forrest et al., 2008, 2011).

Apparently, VGLUT possesses only one substrate binding site that changes its relative substrate affinities during transition from state I to state II, with the features being optimal for substrate binding and release in the two transport modes. In the SV orientation, glutamate is preferred as a substrate over P_i and chloride (open conformational state I). In the plasma membrane orientation (conformational state II), P_i is preferred as substrate over Cl^- and glutamate (P_i > Glut >>> Cl^-). Net P_i transport critically depends on the co-binding of Na^+. The cation binding site or sites in state II appear to be restricted to Na^+ ions, although it remains to be established whether they are related to the cytoplasmic K^+/H^+ binding site characterized previously (Eriksen et al., 2016;

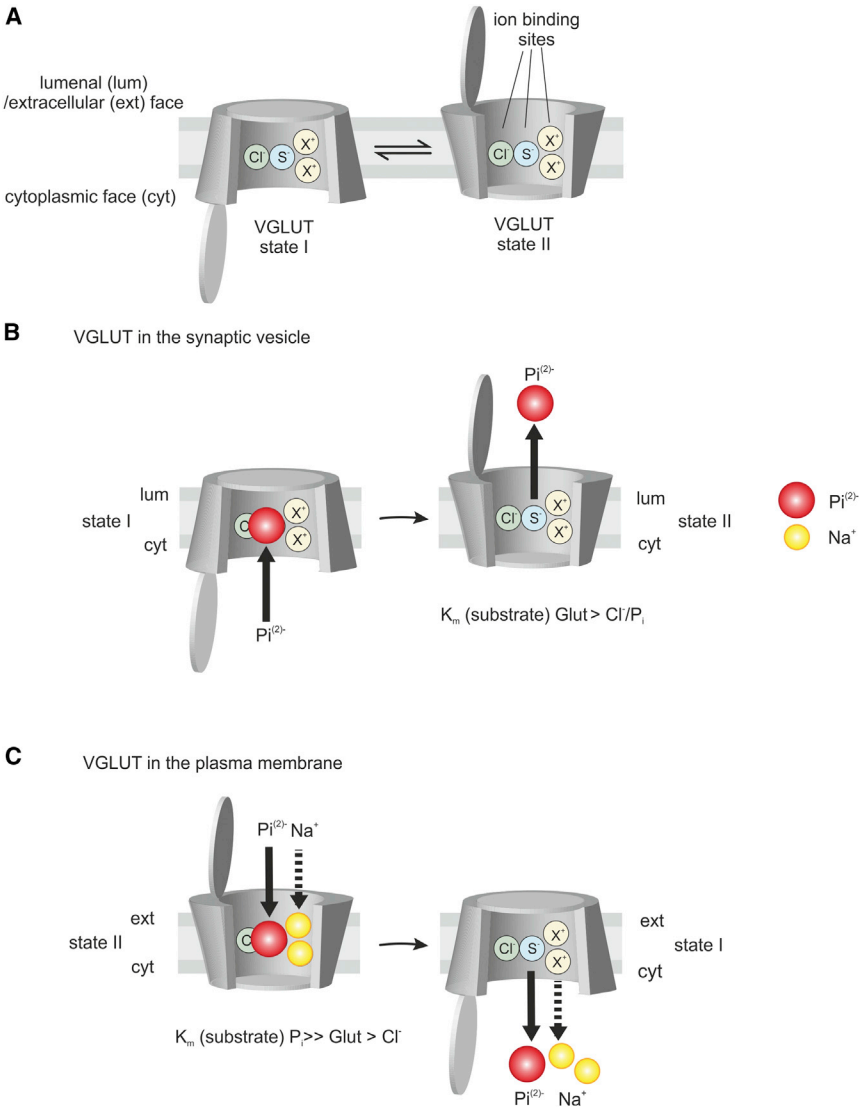

Figure 7. Model of Dual and Direction-Selective Mechanisms of Phosphate Transport by VGLUT
See text for details.

Preobraschenski et al., 2014). Sodium and phosphate transport by cultured neurons (Glinn et al., 1995) or by type II NaP_i transporters expressed in *Xenopus* oocytes is reduced at lower pH, possibly due to competition between Na^+ and H^+ for a common cation binding site (Amstutz et al., 1985; Busch et al., 1996; Murer et al., 2000). Such competition may be relevant for SV after endocytosis: despite containing endocytosed Na^+ and P_i, continued P_i export into the cytoplasm may be prevented due to the acidification of the vesicle interior (Egashira et al., 2015; Farsi et al., 2016; Miesenböck et al., 1998). Our findings disagree with a previous study in which a similar reconstitution approach was used but two separate substrate binding sites were postulated (Juge et al., 2006). We presently have no explanation for this discrepancy.

Overall, the strong preference for P_i over chloride explains why VGLUT, when localized in the plasma membrane, effectively accumulates P_i despite high extracellular Cl^- concentrations, as shown previously in cultured neurons (Glinn et al., 1995) and synaptosomes (Furman et al., 1997) and here in VGLUT1-transfected PC12 cells. Contrary to chloride, the extracellular concentration of glutamate is very low and thus unlikely to affect P_i transport. In contrast, it is unlikely that $\Delta\mu H^+$-driven P_i transport into SV is playing a major role under physiological conditions. Cytoplasmic glutamate concentrations are estimated to be in the range of ~10–20 mM (Shupliakov et al., 1992), greatly exceeding cytoplasmic P_i (~1–5 mM) (Banerjee et al., 2015; Iles et al., 1985). Considering further that glutamate is preferred over P_i in state I, it is evident that glutamate uptake is strongly favored in this mode.

Our findings reveal similarities between VGLUTs and the structurally related type I NaP_i transporters of the SLC17 family, which differ from the type II (SLC34) and type III (SLC20) NaP_i transporters. For instance, VGLUT uses a coupling stoichiometry of $\geq 2\ Na^+$:1 P_i and is driven by the inside negative membrane potential, which is similar to another type I NaP_i family member (Busch et al., 1996). Other type I NaP_i transporters exhibit channel-like chloride conductances that are sensitive to the chloride channel blocker DIDS (4,4'-diisothiocyano-2,2'-stilbenedisulfonic acid) (Busch et al., 1996). In the SV orientation, VGLUT possesses chloride permeability (Eriksen et al., 2016; Preobraschenski et al., 2014; Schenck et al., 2009), and glutamate uptake is highly sensitive to DIDS (Hartinger and Jahn, 1993), raising the possibility that the transporter may also convey a chloride conductance when localized to the plasma membrane.

In conclusion, we show here that the two hitherto incompatible transport activities assigned to the vesicular glutamate transporter VGLUT1 can be integrated into a coherent mechanistic model. Our findings explain how one transporter can have a dual role in synapses: replenishing SV with the neurotransmitter glutamate after endocytotic recovery and importing P_i from the extracellular fluid when residing in the plasma membrane. It remains to be established whether the other VGLUT variants (VGLUT2 and VGLUT3) exhibit similar transport characteristics and whether the transport mechanisms of the other members of the SLC17 subfamily can also operate in different modes.

EXPERIMENTAL PROCEDURES

Animals

Adult Wistar rats were purchased from Charles River Laboratories, or Janvier, and were kept until use at a 12:12 hr light/dark cycle with food and water *ad libitum*. Certificate of approval for using animals was issued by the Landkreis Göttingen Office of Veterinary Affairs and Consumer Protection.

PC12 Cells

PC12 cell lines stably expressing either murine VGLUT1 or transfected with an empty vector (mock) (gift from Prof. Lutz Birnbaumer) were cultivated in DMEM + 10% fetal calf serum (FCS) under 10% CO_2 at 37°C.

Membrane Isolation

SVs (lysis pellet 2 [LP2] and SV fraction) were isolated according to previous publications from rat brains (Huttner et al., 1983; Nagy et al., 1976; Takamori et al., 2006). SVs were collected from the precleared supernatant after lysis by ultracentrifugation (LP2). This pellet is highly enriched in SVs and was used for neurotransmitter uptake (Zander et al., 2010) and hybrid SV formation without further purification. For the radioactive phosphorus isotope ($^{33}P_i$) uptake and acridine orange experiments, the LP2 fraction was further purified by sucrose density gradient centrifugation and size exclusion chromatography (SV fraction).

Expression and Purification of Recombinant Proteins and Nanobodies

VGLUT1 was expressed in insect cells using the baculovirus expression system (Hitchman et al., 2009; Luckow et al., 1993; Smith et al., 1983) and purified following a previously described protocol (Preobraschenski et al., 2014). The plasmid carrying TF_oF_1 with a hexahistidine (His_6)-tagged β subunit (provided by M. Yoshida) (Suzuki et al., 2002) was expressed in *E. coli* DK8 and purified as published previously (Preobraschenski et al., 2014). The ΔN complex consisting of syntaxin-1A (183–288), the C-terminal fragment of synaptobrevin 2 (49–96), and His_6-tagged synaptosomal-associated protein 25 A (SNAP-25A) was expressed and purified as described (Pobbati et al., 2006; Stein et al., 2007). A vector carrying C-terminally His_6-tagged anti-VGLUT1 nanobody 9 was purified following a protocol described in detail in Schenck et al. (2017). Detailed protocols are provided in the Supplemental Experimental Procedures.

Preparation of Proteoliposomes and Generation of Hybrid Vesicles

Proteoliposomes were generated by detergent removal via dialysis of a mixture of the detergent-solubilized components (Rigaud and Lévy, 2003; Rigaud et al., 1995) as previously described (Preobraschenski et al., 2014). The liposomes were composed of 1,2-dioleoyl-*sn*-glycero-3-phosphocholine (DOPC), 1,2-dioleoyl-*sn*-glycero-3-phospho-L-serine (DOPS), and cholesterol (Chol) (from sheep wool) (Avanti Polar Lipids) at a molar ratio of DOPC:DOPS:Chol 65:10:25. The protein:lipid ratio (mol/mol) was adjusted to ~1:40,000 for TF_oF_1, ~1:500 for the ΔN complex, and ~1:2,000 for VGlut1. Hybrid vesicles were generated by fusing TF_oF_1/ΔN or ΔN liposomes with SV for 45 min at room temperature following a protocol previously described (Preobraschenski et al., 2014). For details, see Supplemental Experimental Procedures.

Measurement of ATP and Na^+-Dependent Neurotransmitter and Phosphate Uptake, ΔpH

ATP-dependent glutamate uptake was performed as previously published (Hell et al., 1990; Maycox et al., 1988; Takamori et al., 2000). Neurotransmitter uptake in Figures 1A, 2A, 2B, S1A, and S1B was performed according to Winter et al. (2005) and Zander et al. (2010). Na^+-dependent P_i and glutamate uptake was measured with 2 μCi $^{33}P_i$-phosphoric acid or ^{3}H-glutamic acid (Hartmann Analytik) per data point at 500 μM P_i or Na-glutamate and 3 nM valinomycin for 1 min at 32°C. Acidification measurements were performed according to previous publications (Hell et al., 1990; Maycox et al., 1988) using acridine orange (AO) (Molecular Probes) as a pH-sensitive dye (Palmgren, 1991). Additional experimental details are provided in the Supplemental Experimental Procedures.

Phosphate Uptake by PC12 Cells

PC12 cell lines stably expressing either murine VGLUT1 or transfected with an empty vector (mock) (gift from Prof. Lutz Birnbaumer) were used for determination of phosphate uptake at the plasma membrane using a malachite green and molybdate assay (Biomol green, BML-AK111). For details, see Supplemental Experimental Procedures.

Quantification and Statistical Analysis

For all neurotransmitter and P_i uptake experiments, mean values are plotted, with circles indicating individual data points or error bars representing the range covered by the data points unless indicated otherwise. n indicates the number of independent experiments. For experiments with $n > 4$, data were analyzed using a two-tailed paired t test, $^*p < 0.05$, $^{**}p < 0.01$, $^{***}p < 0.001$, and NS (not significant; $p > 0.05$).

SUPPLEMENTAL INFORMATION

Supplemental Information includes Supplemental Experimental Procedures and three figures and can be found with this article online at https://doi.org/10.1016/j.celrep.2018.03.055.

ACKNOWLEDGMENTS

We thank Ursel Ries and Brigitte Barg-Kues for technical assistance and Linda Olsthoorn for help with the graphical abstract. We also thank Raimund Dutzler for providing the anti-VGLUT1 nanobody plasmid. This work was supported by a grant from the Deutsche Forschungsgemeinschaft to R.J. and G.A.-H. (GZ: AH 67/9, JA 377/7-1, and HO 249/44-1).

AUTHOR CONTRIBUTIONS

J.P., C.C., R.J., and G.A.-H. planned the study and wrote the manuscript. J.P., C.C., M.G., J.F.Z., and K.R. performed the experiments. S.S. developed the anti-VGLUT1 nanobody.

DECLARATION OF INTERESTS

The authors declare no competing interests.

Received: June 1, 2017
Revised: February 13, 2018
Accepted: March 14, 2018
Published: April 10, 2018

REFERENCES

Ahnert-Hilger, G., Höltje, M., Pahner, I., Winter, S., and Brunk, I. (2003). Regulation of vesicular neurotransmitter transporters. Rev. Physiol. Biochem. Pharmacol. *150*, 140–160.

Aihara, Y., Mashima, H., Onda, H., Hisano, S., Kasuya, H., Hori, T., Yamada, S., Tomura, H., Yamada, Y., Inoue, I., et al. (2000). Molecular cloning of a novel brain-type Na(+)-dependent inorganic phosphate cotransporter. J. Neurochem. *74*, 2622–2625.

Amstutz, M., Mohrmann, M., Gmaj, P., and Murer, H. (1985). Effect of pH on phosphate transport in rat renal brush border membrane vesicles. Am. J. Physiol. *248*, F705–F710.

Banerjee, S., Versaw, W.K., and Garcia, L.R. (2015). Imaging Cellular Inorganic Phosphate in Caenorhabditis elegans Using a Genetically Encoded FRET-Based Biosensor. PLoS ONE *10*, e0141128.

Bellocchio, E.E., Reimer, R.J., Fremeau, R.T., Jr., and Edwards, R.H. (2000). Uptake of glutamate into synaptic vesicles by an inorganic phosphate transporter. Science *289*, 957–960.

Busch, A.E., Schuster, A., Waldegger, S., Wagner, C.A., Zempel, G., Broer, S., Biber, J., Murer, H., and Lang, F. (1996). Expression of a renal type I sodium/phosphate transporter (NaP_i-1) induces a conductance in Xenopus oocytes

permeable for organic and inorganic anions. Proc. Natl. Acad. Sci. USA *93*, 5347–5351.

Drew, D., and Boudker, O. (2016). Shared Molecular Mechanisms of Membrane Transporters. Annu. Rev. Biochem. *85*, 543–572.

Edwards, R.H. (2007). The neurotransmitter cycle and quantal size. Neuron *55*, 835–858.

Egashira, Y., Takase, M., and Takamori, S. (2015). Monitoring of vacuolar-type H+ ATPase-mediated proton influx into synaptic vesicles. J. Neurosci. *35*, 3701–3710.

Eriksen, J., Chang, R., McGregor, M., Silm, K., Suzuki, T., and Edwards, R.H. (2016). Protons Regulate Vesicular Glutamate Transporters through an Allosteric Mechanism. Neuron *90*, 768–780.

Farsi, Z., Preobraschenski, J., van den Bogaart, G., Riedel, D., Jahn, R., and Woehler, A. (2016). Single-vesicle imaging reveals different transport mechanisms between glutamatergic and GABAergic vesicles. Science *351*, 981–984.

Farsi, Z., Jahn, R., and Woehler, A. (2017). Proton electrochemical gradient: Driving and regulating neurotransmitter uptake. BioEssays *39*, 1600240.

Forrest, L.R., and Rudnick, G. (2009). The rocking bundle: a mechanism for ion-coupled solute flux by symmetrical transporters. Physiology (Bethesda) *24*, 377–386.

Forrest, L.R., Zhang, Y.W., Jacobs, M.T., Gesmonde, J., Xie, L., Honig, B.H., and Rudnick, G. (2008). Mechanism for alternating access in neurotransmitter transporters. Proc. Natl. Acad. Sci. USA *105*, 10338–10343.

Forrest, L.R., Krämer, R., and Ziegler, C. (2011). The structural basis of secondary active transport mechanisms. Biochim. Biophys. Acta *1807*, 167–188.

Forster, I., Hernando, N., Biber, J., and Murer, H. (1998). The voltage dependence of a cloned mammalian renal type II Na^+/P_i cotransporter (NaP_i-2). J. Gen. Physiol. *112*, 1–18.

Forster, I.C., Hernando, N., Biber, J., and Murer, H. (2013). Phosphate transporters of the SLC20 and SLC34 families. Mol. Aspects Med. *34*, 386–395.

Furman, S., Lichtstein, D., and Ilani, A. (1997). Sodium-dependent transport of phosphate in neuronal and related cells. Biochim. Biophys. Acta *1325*, 34–40.

Glinn, M., Ni, B., and Paul, S.M. (1995). Characterization of Na(+)-dependent phosphate uptake in cultured fetal rat cortical neurons. J. Neurochem. *65*, 2358–2365.

Goh, G.Y., Huang, H., Ullman, J., Borre, L., Hnasko, T.S., Trussell, L.O., and Edwards, R.H. (2011). Presynaptic regulation of quantal size: K+/H+ exchange stimulates vesicular glutamate transport. Nat. Neurosci. *14*, 1285–1292.

Grønborg, M., Pavlos, N.J., Brunk, I., Chua, J.J., Münster-Wandowski, A., Riedel, D., Ahnert-Hilger, G., Urlaub, H., and Jahn, R. (2010). Quantitative comparison of glutamatergic and GABAergic synaptic vesicles unveils selectivity for few proteins including MAL2, a novel synaptic vesicle protein. J. Neurosci. *30*, 2–12.

Hartinger, J., and Jahn, R. (1993). An anion binding site that regulates the glutamate transporter of synaptic vesicles. J. Biol. Chem. *268*, 23122–23127.

Hell, J.W., Maycox, P.R., and Jahn, R. (1990). Energy dependence and functional reconstitution of the gamma-aminobutyric acid carrier from synaptic vesicles. J. Biol. Chem. *265*, 2111–2117.

Hitchman, R.B., Possee, R.D., and King, L.A. (2009). Baculovirus expression systems for recombinant protein production in insect cells. Recent Pat. Biotechnol. *3*, 46–54.

Huttner, W.B., Schiebler, W., Greengard, P., and De Camilli, P. (1983). Synapsin I (protein I), a nerve terminal-specific phosphoprotein. III. Its association with synaptic vesicles studied in a highly purified synaptic vesicle preparation. J. Cell Biol. *96*, 1374–1388.

Iles, R.A., Stevens, A.N., Griffiths, J.R., and Morris, P.G. (1985). Phosphorylation status of liver by ^{31}P-n.m.r. spectroscopy, and its implications for metabolic control. A comparison of ^{31}P-n.m.r. spectroscopy (*in vivo* and *in vitro*) with chemical and enzymic determinations of ATP, ADP and P_i. Biochem. J. *229*, 141–151.

Juge, N., Yoshida, Y., Yatsushiro, S., Omote, H., and Moriyama, Y. (2006). Vesicular glutamate transporter contains two independent transport machineries. J. Biol. Chem. *281*, 39499–39506.

Juge, N., Gray, J.A., Omote, H., Miyaji, T., Inoue, T., Hara, C., Uneyama, H., Edwards, R.H., Nicoll, R.A., and Moriyama, Y. (2010). Metabolic control of vesicular glutamate transport and release. Neuron *68*, 99–112.

Krishnamurthy, H., Piscitelli, C.L., and Gouaux, E. (2009). Unlocking the molecular secrets of sodium-coupled transporters. Nature *459*, 347–355.

Luckow, V.A., Lee, S.C., Barry, G.F., and Olins, P.O. (1993). Efficient generation of infectious recombinant baculoviruses by site-specific transposon-mediated insertion of foreign genes into a baculovirus genome propagated in *Escherichia coli*. J. Virol. *67*, 4566–4579.

Maycox, P.R., Deckwerth, T., Hell, J.W., and Jahn, R. (1988). Glutamate uptake by brain synaptic vesicles. Energy dependence of transport and functional reconstitution in proteoliposomes. J. Biol. Chem. *263*, 15423–15428.

Miesenböck, G., De Angelis, D.A., and Rothman, J.E. (1998). Visualizing secretion and synaptic transmission with pH-sensitive green fluorescent proteins. Nature *394*, 192–195.

Murer, H., Hernando, N., Forster, I., and Biber, J. (2000). Proximal tubular phosphate reabsorption: molecular mechanisms. Physiol. Rev. *80*, 1373–1409.

Nagy, A., Baker, R.R., Morris, S.J., and Whittaker, V.P. (1976). The preparation and characterization of synaptic vesicles of high purity. Brain Res. *109*, 285–309.

Naito, S., and Ueda, T. (1985). Characterization of glutamate uptake into synaptic vesicles. J. Neurochem. *44*, 99–109.

Ni, B., Rosteck, P.R., Jr., Nadi, N.S., and Paul, S.M. (1994). Cloning and expression of a cDNA encoding a brain-specific Na(+)-dependent inorganic phosphate cotransporter. Proc. Natl. Acad. Sci. USA *91*, 5607–5611.

Omote, H., Miyaji, T., Juge, N., and Moriyama, Y. (2011). Vesicular neurotransmitter transporter: bioenergetics and regulation of glutamate transport. Biochemistry *50*, 5558–5565.

Orlowski, J., and Grinstein, S. (2004). Diversity of the mammalian sodium/proton exchanger SLC9 gene family. Pflugers Arch. *447*, 549–565.

Palmgren, M.G. (1991). Acridine orange as a probe for measuring pH gradients across membranes: mechanism and limitations. Anal. Biochem. *192*, 316–321.

Parker, J.L., Mindell, J.A., and Newstead, S. (2014). Thermodynamic evidence for a dual transport mechanism in a POT peptide transporter. eLife *3*, e04273.

Pobbati, A.V., Stein, A., and Fasshauer, D. (2006). N- to C-terminal SNARE complex assembly promotes rapid membrane fusion. Science *313*, 673–676.

Preobraschenski, J., Zander, J.F., Suzuki, T., Ahnert-Hilger, G., and Jahn, R. (2014). Vesicular glutamate transporters use flexible anion and cation binding sites for efficient accumulation of neurotransmitter. Neuron *84*, 1287–1301.

Rigaud, J.L., and Lévy, D. (2003). Reconstitution of membrane proteins into liposomes. Methods Enzymol. *372*, 65–86.

Rigaud, J.L., Pitard, B., and Levy, D. (1995). Reconstitution of membrane proteins into liposomes: application to energy-transducing membrane proteins. Biochim. Biophys. Acta *1231*, 223–246.

Schenck, S., Wojcik, S.M., Brose, N., and Takamori, S. (2009). A chloride conductance in VGLUT1 underlies maximal glutamate loading into synaptic vesicles. Nat. Neurosci. *12*, 156–162.

Schenck, S., Kunz, L., Sahlender, D., Pardon, E., Geertsma, E.R., Savtchouk, I., Suzuki, T., Neldner, Y., Štefanić, S., Steyaert, J., et al. (2017). Generation and Characterization of Anti-VGLUT Nanobodies Acting as Inhibitors of Transport. Biochemistry *56*, 3962–3971.

Shupliakov, O., Brodin, L., Cullheim, S., Ottersen, O.P., and Storm-Mathisen, J. (1992). Immunogold quantification of glutamate in two types of excitatory synapse with different firing patterns. J. Neurosci. *12*, 3789–3803.

Smith, G.E., Fraser, M.J., and Summers, M.D. (1983). Molecular Engineering of the Autographa californica Nuclear Polyhedrosis Virus Genome: Deletion Mutations Within the Polyhedrin Gene. J. Virol. *46*, 584–593.

Stein, A., Radhakrishnan, A., Riedel, D., Fasshauer, D., and Jahn, R. (2007). Synaptotagmin activates membrane fusion through a Ca2+-dependent trans interaction with phospholipids. Nat. Struct. Mol. Biol. *14*, 904–911.

Sudhof, T.C. (2004). The synaptic vesicle cycle. Annu. Rev. Neurosci. *27*, 509–547.

Suzuki, T., Ueno, H., Mitome, N., Suzuki, J., and Yoshida, M. (2002). F(0) of ATP synthase is a rotary proton channel. Obligatory coupling of proton translocation with rotation of c-subunit ring. J. Biol. Chem. *277*, 13281–13285.

Tabb, J.S., Kish, P.E., Van Dyke, R., and Ueda, T. (1992). Glutamate transport into synaptic vesicles. Roles of membrane potential, pH gradient, and intravesicular pH. J. Biol. Chem. *267*, 15412–15418.

Takamori, S. (2016). Presynaptic Molecular Determinants of Quantal Size. Front. Synaptic Neurosci. *8*, 2.

Takamori, S., Rhee, J.S., Rosenmund, C., and Jahn, R. (2000). Identification of a vesicular glutamate transporter that defines a glutamatergic phenotype in neurons. Nature *407*, 189–194.

Takamori, S., Holt, M., Stenius, K., Lemke, E.A., Grønborg, M., Riedel, D., Urlaub, H., Schenck, S., Brügger, B., Ringler, P., et al. (2006). Molecular anatomy of a trafficking organelle. Cell *127*, 831–846.

Winter, S., Brunk, I., Walther, D.J., Höltje, M., Jiang, M., Peter, J.U., Takamori, S., Jahn, R., Birnbaumer, L., and Ahnert-Hilger, G. (2005). Galphao2 regulates vesicular glutamate transporter activity by changing its chloride dependence. J. Neurosci. *25*, 4672–4680.

Wolosker, H., de Souza, D.O., and de Meis, L. (1996). Regulation of glutamate transport into synaptic vesicles by chloride and proton gradient. J. Biol. Chem. *271*, 11726–11731.

Zander, J.F., Münster-Wandowski, A., Brunk, I., Pahner, I., Gómez-Lira, G., Heinemann, U., Gutiérrez, R., Laube, G., and Ahnert-Hilger, G. (2010). Synaptic and vesicular coexistence of VGLUT and VGAT in selected excitatory and inhibitory synapses. J. Neurosci. *30*, 7634–7645.